# X,Y,Z-Waves: Extended Structures in Nonlinear Lattices

P. G. Kevrekidis[1], J. Gagnon[1], D. J. Frantzeskakis[2] and B. A. Malomed[3]
[1] *Department of Mathematics and Statistics, University of Massachusetts, Amherst MA 01003-4515*
[2] *Department of Physics, University of Athens, Panepistimiopolis, Zografos, Athens 15784, Greece*
[3] *Department of Interdisciplinary Studies, Faculty of Engineering, Tel Aviv University, Tel Aviv 69978, Israel*

Motivated by recent experimental and theoretical results on optical X-waves, we propose a new type of waveforms in 2D and 3D discrete media – multi-legged extended nonlinear structures (ENS), built as arrays of lattice solitons (*tiles* or *stones*, in the 2D and 3D cases, respectively). First, we study the stability of the tiles and stones analytically, and then extend them numerically to complete ENS forms for both 2D and 3D lattices. The predicted patterns are relevant to a variety of physical settings, such as Bose-Einstein condensates in deep optical lattices, lattices built of microresonators, photorefractive crystals with optically induced lattices (in the 2D case) and others.

*Introduction and setup.* In the past few years, studies of dynamics in discrete media, as well as in their continuum periodically modulated counterparts, have enjoyed very rapid progress [1]. This is fueled by a need to tackle diverse physical contexts such as nonlinear optics of waveguide arrays and photorefractive crystals [2], the physics of Bose-Einstein condensates (BECs) in optical lattices [3], the denaturation of the DNA double-strand [4], and so on. These efforts have resulted in the creation of a variety of novel nonlinear structures, such as discrete dipole [5], quadrupole [6], necklace [7] and other multi-pulse/multi-pole localized patterns [8], discrete vortices [9], ring solitons [10], and others [11]. Such structures have a potential to be used as carriers and conduits for data transmission and processing, in the context of all-optical and quantum-information schemes.

The present work is motivated by the above-mentioned achievements, as well as by recent developments in studies of *X-waves*, which are quasi-linear extended structures generated in three-dimensions (3D) [12], two-dimensions (2D) [13], and even quasi-discrete [14] media. These waves arise when the linear second-order differential operator in the relevant wave equation is genuinely, or effectively [15], sign-indefinite (roughly speaking, a D'Alembertian instead of the Laplacian). A similar shape is featured by cross configurations formed by two intersecting domain walls in a system of two coupled 2D Gross-Pitaevskii equations [16], with a difference that these structure are essentially nonlinear ones.

In the present work, we are dealing with the sign-definite discrete Laplacian (nevertheless, one can easily induce the sign-indefiniteness in the discrete wave equation, applying the well-known *staggering transformation* [1] along one coordinate only). Instead of emulating the mathematical structure of the continuous wave equations supporting X-waves in the lattice medium, our aim is to construct stable extended nonlinear structures (ENSs) in *discrete* media. These wave structures are partly delocalized, by their nature, ranging from a few sites to infinitely extended ones. An essential difference between the quasi-linear X-waves in continua and the lattice entities presented here is that the latter are *strongly nonlinear* structures, being built as arrays of individual lattice solitons ("tiles"); in that sense, they somewhat resemble weakly localized *hypersolitons* [17] and *supervortices* [18], constructed as finite ensembles of individual solitons. In fact, we initialize our analysis (see below) from a purely nonlinear (*anti-continuum*, AC) limit, without linear intersite coupling on the lattice. The eventual shape of the extended lattice waves features a great variety, including X-waves, Y-waves, Z-waves and other forms, provided that the underlying core ("tile") is dynamically stable. Each species is stable in a finite interval of values of the intersite coupling constant. Some of those patterns may definitely be of interest (for instance, as star-shaped waveguiding configurations) to applications in both nonlinear-optical and matter-wave contexts, where they can potentially be created.

The analysis is performed in terms of the discrete nonlinear Schrödinger (DNLS) equation in 2D or 3D,

$$i\dot{u}_{\mathbf{n}} = -\epsilon\left(\Delta_2 u\right)_{\mathbf{n}} - |u_{\mathbf{n}}|^2 u_{\mathbf{n}}, \tag{1}$$

where $u_{\mathbf{n}}$ is a complex amplitude of the electromagnetic wave in an optical waveguide array (in the 2D case) [2, 19], or the BEC wave function at nodes of a deep (2D or 3D) optical lattice [20], $\mathbf{n}$ being the vectorial lattice index, and $\Delta_2$ the standard discrete Laplacian. Further, $\epsilon$ is the constant of the intersite coupling, and the overdot stands for the derivative with respect to the evolution variable; the latter is $z$ in optical arrays, or $t$ in the BEC model (or in a crystal built of microresonators [21]).

The presentation of our results on ENS solutions of Eq. (1) proceeds as follows. First, in the AC limit ($\epsilon = 0$), we specify main types of the "tiles", of which the ENSs are to be composed. Then, we numerically extend these compositions into full ENS solutions for $\epsilon > 0$. Finally, we summarize our findings and discuss further problems.

*Analytical results: tiles, stones, and their stability.* We look for standing-wave solutions to Eq. (1), in the form of $u_{\mathbf{n}} = \exp(i\Lambda t)\phi_{\mathbf{n}}$, with $\phi_{\mathbf{n}}$ satisfying the equation,

$$f(\phi_{\mathbf{n}}, \epsilon) = \Lambda\phi_{\mathbf{n}} - \epsilon\Delta_2\phi_{\mathbf{n}} - |\phi_{\mathbf{n}}|^2\phi_{\mathbf{n}} = 0. \tag{2}$$

Perturbation of Eq. (1) around the solutions of Eq. (2) leads to the linearization operator,

$$\mathcal{H}_{\mathbf{n}}^{(\epsilon)} = \begin{pmatrix} \Lambda - 2|\phi_{\mathbf{n}}|^2 & -\phi_{\mathbf{n}}^2 \\ -\bar{\phi}_{\mathbf{n}}^2 & \Lambda - 2|\phi_{\mathbf{n}}|^2 \end{pmatrix} - \epsilon\Delta_2 \begin{pmatrix} 1 & 0 \\ 0 & 1 \end{pmatrix}, \tag{3}$$

the overbar standing for complex conjugate. By means of a rescaling, we fix $\Lambda \equiv 1$, keeping $\epsilon$ as a free parameter.

In the AC limit of $\epsilon = 0$, solutions to Eq. (2) are $u_{\mathbf{n}} = re^{i\theta_{\mathbf{n}}}$, where real amplitude $r$ is 0 or $\sqrt{\Lambda}$, and $\theta_{\mathbf{n}}$ are arbitrary constants. To continue such a solution to $\epsilon \neq 0$, the Lyapunov-Schmidt condition needs to be satisfied [22], *viz.*, the projection of eigenvectors of the kernel of $\mathcal{H}^{(0)}_{\mathbf{n}}$ (i.e., zero modes of the operator) onto the system of stationary equations should be null. This condition gives rise to a solvability condition at each "AC-filled" site, i.e., one with $r \neq 0$ in the AC limit,

$$-2ig_{\mathbf{n}}(\theta,\epsilon) = \epsilon e^{-i\theta_{\mathbf{n}}}\Delta_2\phi_{\mathbf{n}} - \epsilon e^{i\theta_{\mathbf{n}}}\left(\Delta_2\bar{\phi}\right)_{\mathbf{n}} \qquad (4)$$

(the factor of $-2i$ is introduced for convenience). Importantly, the eigenvalues $\gamma$ of the Jacobian, $\mathcal{M}_{ij} = \partial g_i/\partial\theta_j$, are intimately related to the leading-order approximation for eigenvalues ($\lambda$) of the linearization around a stationary solution, $\lambda = \pm\sqrt{2\gamma}$. We use this relation, alongside a perturbative expansion in the solution, $\phi_{\mathbf{n}} = \phi^{(0)}_{\mathbf{n}} + \epsilon\phi^{(1)}_{\mathbf{n}} + \ldots$, to derive leading-order bifurcation conditions for any given configuration, and subsequently to find the corresponding linear-stability eigenvalues.

2D configurations can be categorized by the number of their "legs" (i.e., the number of quasi-1D lines of excited sites it contains). Simplest is the one-leg structure assembled of two- or three-site tiles, for which 1D stability results are applicable [22]; here, the resulting Jacobian is

$$(\mathcal{M}_1)_{i,j} = \begin{cases} \cos(\theta_{j+1}-\theta_j) + \cos(\theta_{j-1}-\theta_j), & i=j, \\ -\cos(\theta_j - \theta_i), & i = j \pm 1, \\ 0, & |i-j| \geq 2, \end{cases}$$

from which conclusions for the stability of ENSs may be drawn. In particular, a fundamental stability condition extensively used in our analysis is that the phase shift between fields at adjacent sites must be $\pi$ [22, 23]. For the two-site tile satisfying this condition, the stability eigenvalues are [22] $\lambda = \sqrt{2\gamma} = \pm 2\sqrt{\epsilon}i$, while for its three-site counterpart, $(+1,-1,+1)$, they are $\lambda = \pm\sqrt{2\epsilon}i$ and $\lambda = \pm\sqrt{6\epsilon}i$. The full one-leg configuration assembled of these tiles is a chain, $(\ldots,-1,+1,-1,+1,-1,\ldots)$, hereafter termed configuration 1.

Proceeding to two-tile configurations allows us to examine more complex (in particular, X- and Y-like) 2D structures. X-configurations can be built of square- or cross-shaped tiles, which, in the AC limit, are

$$\begin{pmatrix} 1 & 0 & -1 \\ 0 & 0 & 0 \\ -1 & 0 & 1 \end{pmatrix} \text{ and } \begin{pmatrix} 1 & 0 & 1 \\ 0 & -1 & 0 \\ 1 & 0 & 1 \end{pmatrix} \qquad (5)$$

However, the latter one gives rise to an unstable eigenvalue pair, $\lambda = \pm 2\epsilon$ (to leading order), therefore it is not considered further. The former tile has a pair of $\lambda = \pm 2\sqrt{2}\epsilon i$, and a double one, $\lambda = \pm 2\epsilon i$, hence stable X-configurations (to be called 2a) can be constructed at finite $\epsilon$ as arrays of such tiles with alternating signs.

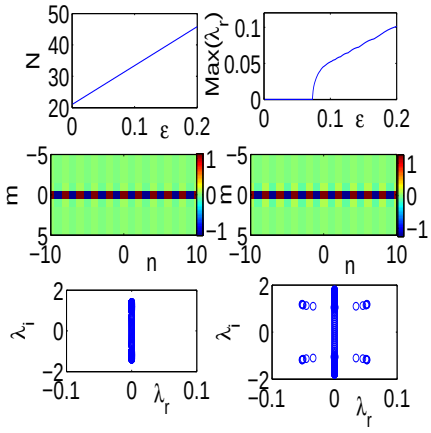

FIG. 1: (Color online) A family of single-leg patterns in the 2D DNLS equation. The top left and right panels show, respectively, the norm and the largest instability growth rate vs. $\epsilon$. The contour plots in the middle panels show the stationary solutions for $\epsilon = 0.05$ (stable) and $\epsilon = 0.1$ (unstable). The spectral planes $(\lambda_r, \lambda_i)$ of numerically computed eigenvalues for these solutions are displayed in the bottom panels.

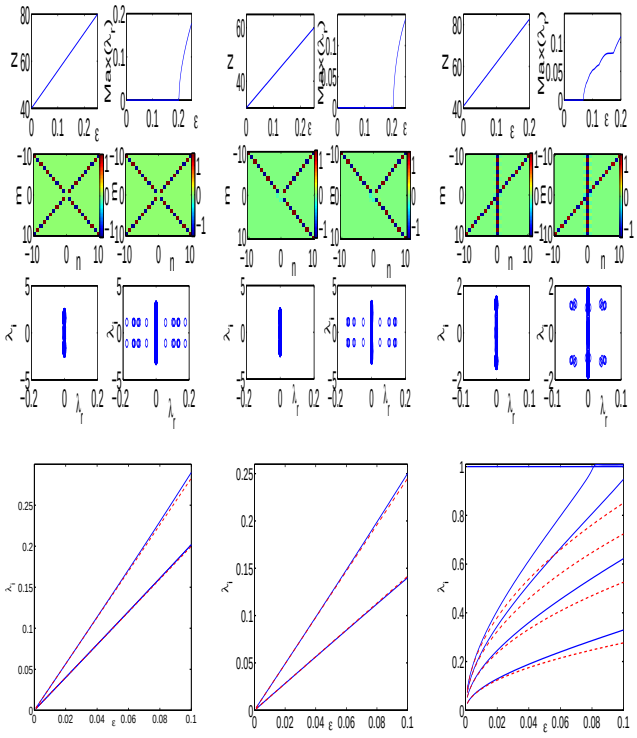

FIG. 2: Same as in Fig. 1 but for configurations 2a, 2b and 2c. Bottom panels present the stability eigenvalues for individual tiles of which these patterns are built, numerically found ones (solid lines) versus the analytical prediction (dashed lines). Examples of species 2a and 2b are displayed in two left and two middle panels for $\epsilon = 0.15$ and 0.25, and an example of 2c in the right panels pertain to $\epsilon = 0.05$ and $\epsilon = 0.1$.

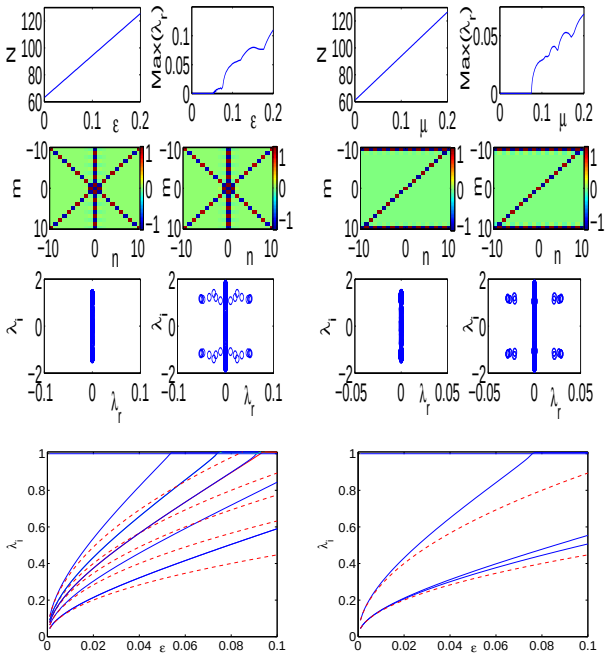

FIG. 3: Same as Fig. 2, but for configurations 3a and 3b. Examples of both species are shown for $\epsilon = 0.05$ and 0.1.

Other two-leg configurations are Y-shaped and "skew-X" ones, composed, respectively, of the tiles:

$$\begin{pmatrix} 1 & 0 & -1 \\ 0 & 0 & 0 \\ 0 & 0 & 1 \end{pmatrix} \text{ and } \begin{pmatrix} 0 & -1 & 1 \\ 0 & 1 & 0 \\ 1 & -1 & 0 \end{pmatrix}. \qquad (6)$$

Both these tiles are stable, with respective eigenvalues $\lambda = \pm\sqrt{2\epsilon}i$ and $\lambda = \pm\sqrt{6\epsilon}i$ for the former, and $\lambda = \pm 0.874\sqrt{\epsilon}i$, $\lambda = \pm 1.663\sqrt{\epsilon}i$, $\lambda = \pm 2.882\sqrt{\epsilon}i$ and $\lambda = \pm 2.690\sqrt{\epsilon}i$ for the latter. Stable sign-alternate ENSs assembled of them are termed 2b and 2c, respectively.

Three-leg ENSs can be built of other (generally, denser filled) *stable* tiles, such as

$$\begin{pmatrix} 1 & -1 & 1 \\ -1 & 1 & -1 \\ 1 & -1 & 1 \end{pmatrix} \text{ and } \begin{pmatrix} 1 & -1 & 1 \\ 0 & 1 & 0 \\ -1 & 0 & 0 \end{pmatrix}. \qquad (7)$$

The former tile possesses three pairs of double eigenvalues, $\pm\sqrt{2\epsilon}i$, $\pm\sqrt{6\epsilon}i$, and $\pm\sqrt{8\epsilon}i$, and two pairs of single ones, $\pm 2\sqrt{\epsilon}i$ and $\pm\sqrt{12\epsilon}i$. The latter has a double eigenvalue $\pm\sqrt{2\epsilon}i$ and a single one $\pm\sqrt{8\epsilon}i$. Three-leg configurations constructed of these tiles with alternating signs are called 3a and 3b, see below. In fact, the latter one will be a Z-shaped array.

Finally, we consider two configurations as a proof-of-principle of the extension of the ENS concept to the 3D space. In particular, augmenting the first tile of (7) by two $-1$ sites, adjacent to middle 1 along the third direction, we fabricate a "stone". The stone is stable, with single eigenvalues $\lambda = \pm 1.248\sqrt{\epsilon}i$, $\lambda = \pm 2\sqrt{\epsilon}i$, $\lambda = \pm\sqrt{6\epsilon}i$, $\lambda = \pm 2.763\sqrt{\epsilon}i$ and $\lambda = \pm 3.848\sqrt{\epsilon}i$, and double and

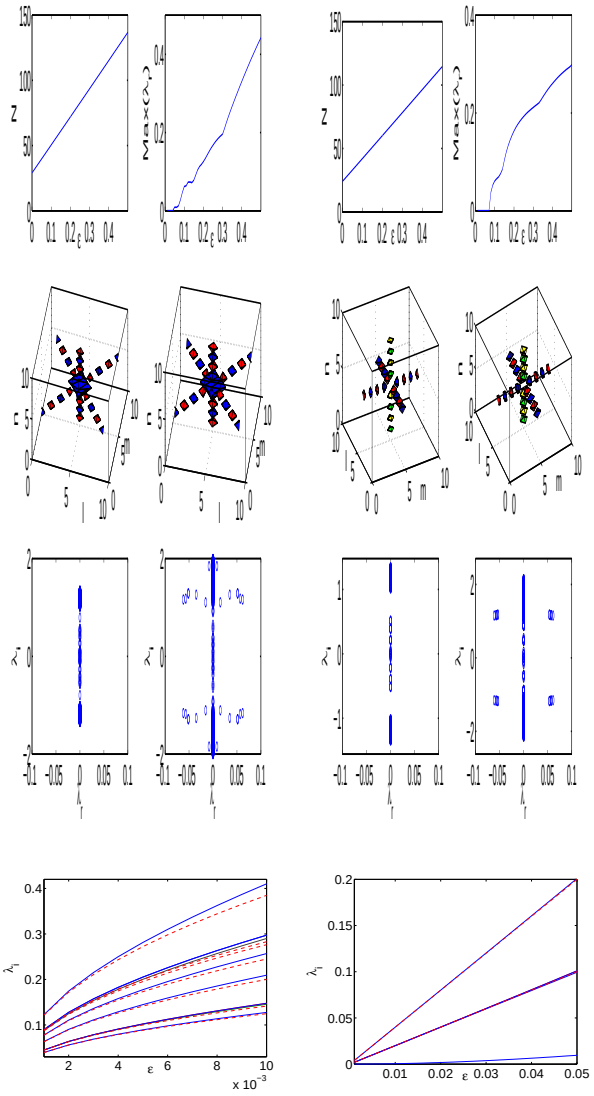

FIG. 4: Same as in above figures, but for 3D configurations 4a and 4b. Their examples are plotted, in two left and two right panels, respectively, for $\epsilon = 0.03$ and $\epsilon = 0.1$. In configuration 4b, the imaginary parts are shown by different colors, green for phase $\pi/2$ and yellow for $3\pi/2$.

triple ones, $\lambda = \pm\sqrt{8\epsilon}i$ and $\lambda = \pm\sqrt{2\epsilon}i$, respectively. These stones will be used to build a stable 3D pattern (again, with sign alternations), called 4a in our nomenclature.

The simplest stable stone has a "diamond"-like shape, i.e., it consists of six AC-filled sites surrounding, as nearest neighbors, an empty one. Although some configurations of this type are unstable [11], we have found a stable one, carrying a phase distribution that corresponds to a quadrupole in the plane, with phases $\pi/2$ and $3\pi/2$ lent to the two out-of-plane sites. This stone has triple and single eigenvalues, $\lambda = \pm 2\epsilon i$ and $\lambda = \pm 4\epsilon i$, respectively,

and a higher-order one, $\mathcal{O}(\epsilon^2)$. Augmenting stones of this type by alternating phase pulses, we will build a stable 3D structure labeled 4b.

*Numerical results.* In Figs. 1-4 we present, in a unified format, results of the numerical continuation of various ENS configurations from the AC limit. Figure 1 shows configuration 1 (a straight chain of sign-alternating tiles). The norm of the configuration, $N = \sum_n \phi_n^2$, and its maximum instability growth rate are shown, as a function of $\epsilon$, in the top left and right panel, respectively. In the 21x21 lattice used in our 2D computation, the configuration becomes unstable for $\epsilon > 0.074$. The middle panels show typical examples of stable and unstable configurations, and the bottom panels show the spectral plane $(\lambda_r, \lambda_i)$ of their numerically found (in)stability eigenvalues, $\lambda \equiv \lambda_r + i\lambda_i$, the instability being ushered by $\lambda_r \neq 0$.

Figure 2 presents three different varieties of the two-leg configurations: 2a (X-waves, left panels), 2b (Y-waves, middle panels) and 2c (skewed X-waves, right panels). In addition, numerically computed stability eigenvalues of the corresponding tiles, i.e., the first one in Eq. (5) and both in Eq. (6), are shown by solid blue lines for comparison with the analytical predictions of the previous section (dashed red lines), indicating good agreement between them. Configurations 2a, 2b, and 2c become unstable at $\epsilon > 0.202$, $\epsilon \geq 0.206$ and $\epsilon \geq 0.068$ respectively.

Similarly, Fig. 3 shows two three-leg configurations, 3a and 3b (the latter one may be naturally called a Z-wave), and their stability characteristics. These configurations become unstable at $\epsilon > 0.053$ and $\epsilon \geq 0.075$, respectively.

Finally, figure 4 shows the continuation to $\epsilon \neq 0$ of 3D configurations 4a and 4b (defined above), which are stable, respectively, at $\epsilon \leq 0.043$ and $\epsilon \leq 0.075$. Note that the corresponding numerically computed eigenvalues (for the respective stones) again agree well with the analytical predictions.

*Conclusion.* We have presented a systematic approach towards constructing a variety of extended states on 2D and 3D nonlinear lattices. They are composed of building blocks, namely, tiles (2D) or stones (3D) with alternating signs, that are originally defined in the anti-continuum limit (the sign alternation is necessary for stability of the patterns). Stability intervals for the structures were revealed by numerical continuation of the corresponding solution families to finite values of the coupling constant. Examination of nonlinear evolution of unstable patterns is another relevant problem, to be considered elsewhere.

Another interesting topic is a discrete model such as Eq. (1), but with a negative intersite coupling in one spatial direction (say, $x$); as mentioned above, this model can be generated from Eq. (1) by means of the staggering transformation applied in this direction, i.e., $u_{n_x,n_y,n_z} \equiv (-1)^{n_x} v_{n_x,n_y,n_z}$. In the 2D version of such a model, one can immediately find two exact *linear* single-leg solutions oriented along the diagonals, *viz.*, $u_{n_x,n_y} = \exp(-|n_x \mp n_y|)$. Their superposition can be used to construct exact linear X-waves. A potential extension of the latter states into the nonlinear model would also be worth considering.


[1] S. Aubry, Physica **103D**, 201 (1997); S. Flach and C. R. Willis, Phys. Rep. **295**, 181 (1998); D. K. Campbell, S. Flach, and Y. S. Kivshar, Phys. Today, January 2004, p. 43.

[2] D. N. Christodoulides *et al.*, Nature **424**, 817 (2003); A. A. Sukhorukov *et al.*, IEEE J. Quant. Elect. **39**, 31 (2003). J. W. Fleischer *et al.*, Opt. Express **13**, 1780 (2005).

[3] V. A. Brazhnyi and V. V. Konotop, Mod. Phys. Lett. B **18**, 627 (2004); P. G. Kevrekidis and D. J. Frantzeskakis, Mod. Phys. Lett. B **18**, 173 (2004).

[4] M. Peyrard, Nonlinearity **17**, R1 (2004).

[5] J. Yang *et al.*, Opt. Lett. **29**, 1662 (2004).

[6] J. Yang *et al.*, Stud. Appl. Math. **113**, 389 (2004).

[7] J. Yang *et al.*, Phys. Rev. Lett. **94**, 113902 (2005).

[8] Z. Chen *et al.*, Phys. Rev. Lett. **92**, 143902 (2004).

[9] D. N. Neshev *et al.*, Phys. Rev. Lett. 92, 123903 (2004); J. W. Fleischer *et al.*, Phys. Rev. Lett. **92**, 123904 (2004).

[10] X. Wang, Z. Chen, and P. G. Kevrekidis, Phys. Rev. Lett. **96**, 083904 (2006).

[11] R. Carretero-González *et al.*, Phys. Rev. Lett. **94**, 203901 (2005); T. J. Alexander *et al.*, Phys. Rev. A **72**, 043603 (2005).

[12] J. Y. Lu and J. F. Greenleaf, IEEE Trans. Ultrason. Ferroelectr. Freq. Control **39**, 19 (1992); P. Di Trapani *et al.*, Phys. Rev. Lett. **91**, 093904 (2003). C. Conti *et al.*, Phys. Rev. Lett. **90**, 093904 (2003).

[13] D. N. Christodoulides *et al.*, Opt. Lett. **29**, 1446 (2004).

[14] S. Droulias *et al.*, Opt. Express **13**, 1827 (2005).

[15] C. Conti and S. Trillo, Phys. Rev. Lett. **92**, 120404 (2004).

[16] B. A. Malomed *et al.*, Phys. Rev. A **70**, 043616 (2004).

[17] J. R. Salgueiro, H. Michinel, and M. I. Rodas-Verde., e-print nlin.PS/0603011.

[18] H. Sakaguchi and B. A. Malomed, Europhys. Lett. **72**, 698 (2005).

[19] P. G. Kevrekidis, K. Ø. Rasmussen and A. R. Bishop, Int. J. Mod. Phys. B **15**, 2833 (2001).

[20] A. Trombettoni and A. Smerzi, Phys. Rev. Lett. **86**, 2353 (2001); G. L. Alfimov *et al.*, Phys. Rev. E **66**, 046608 (2002)

[21] J. E. Heebner and R. W. Boyd, J. Mod. Opt. **49**, 2629 (2002); P. Chak *et al.*, Opt. Lett. **28**, 1966 (2003).

[22] D. E. Pelinovsky *et al.*, Physica D **212**, 1 (2005); *ibid.* **212**, 20 (2005).

[23] T. Kapitula, P. G. Kevrekidis, and B.A. Malomed, Phys. Rev. E **63**, 036604 (2001).